Haonan Zhao, Yuanyuan Zhang, Wei Du, Yang Zhang, Renjie Zhou, and Zhaojie Guo, 2022, The Late Triassic Longmenshan lateral foreland thrusting: New insights from geological evidence and 3-D particle discrete-element simulation: GSA Bulletin, https://doi.org/10.1130/B36501.1.

Supplemental Material

Figure S1. The tight folds with sub-vertical axial planes, sub-vertical strata and fault-bend folds. Three profiles were measured to study the dip direction of nearly vertical strata (S0) and the axial planes of the folds (S1).

Figure S2. The average lateral displacement and shortening amount in the X direction of landmarks with different X coordinates in models which have different thickness of material located on the x-axis *h1(x, 0)*, when the rotation angles of compressional blocks are 20°. It is clear that the lateral displacement increases and the division between the extension zone and the compresion zone moves farther away from the blocking block with increasing of the material thickness *h1(x, 0)*. However, the position where the maximum shortening amount appears does not change apparently, suggesting that the margin of the blocking block is always the position where the strongest shortening and thrusting occurs. The effect of the material thickness *h1(x, 0)* on the lateral foreland thrusting revealed by simulation results is in agreement with the numerical analysis.

Figure S3. The lateral topographic gradient β with different internal friction angle φ when the rotation angles are 20°. It is clear that the topographic gradient β is the same as the internal friction angle increases (Fig.S3), which suggests that the internal friction angle has little effect on lateral extrusion.

Figure S4. The average lateral displacement and shortening amount of landmarks with different internal friction angle φ when the rotation angles are 20°. The lateral displacement gets slightly larger as the internal friction angle φ gets larger, except when X = -21.The position where the maximum shortening amount appears does not change apparently, which is still located at the margin of the blocking block (between X = 0 and X = 6 in Fig.S4b). The shortening amount shows no significant difference with various internal friction angle φ.

Table S1. Calcite U-Pb dating results with errors.

Supplemental Material

The Late Triassic Longmenshan lateral foreland thrusting: New insights from geological evidence and 3D particle discrete element simulation

Haonan Zhao[1], Yuanyuan Zhang[1], Wei Du[1],

Yang Zhang[1], Renjie Zhou[2], Zhaojie Guo[1*]

[1]The Key Laboratory of Orogenic Belts and Crustal Evolution, Ministry of Education, School of Earth and Space Sciences, Peking University, Beijing 100871, China.

[2]School of Earth and Environmental Sciences, The University of Queensland, Brisbane, QLD 4072, Australia.

**Corresponding author: zjguo@pku.edu.cn*

SUPPLEMENTAL FILE 1

Figure S1. The tight folds with sub-vertical axial planes, sub-vertical strata and fault-bend folds. Three profiles were measured to study the dip direction of nearly vertical strata (S0) and the axial planes of the folds (S1).

Figure S2. The average lateral displacement and shortening amount in the X direction of landmarks with different X coordinates in models which have different thickness of material located on the x-axis $h_1(x, 0)$, when the rotation angles of compressional blocks are 20°. It is clear that the lateral displacement increases and the division between the extension zone and the compresion zone moves farther away from the blocking block with increasing of the material thickness $h_1(x, 0)$. However, the position where the maximum shortening amount appears does not change apparently, suggesting that the margin of the blocking block is always the position where the strongest shortening and thrusting occurs. The effect of the material thickness $h_1(x, 0)$ on the lateral foreland thrusting revealed by simulation results is in agreement with the numerical analysis.

Figure S3. The lateral topographic gradient β with different internal friction angle φ when the rotation angles are 20°. It is clear that the topographic gradient β is the same as the internal friction angle increases (Fig.S3), which suggests that the internal friction angle has little effect on lateral extrusion.

Figure S4. The average lateral displacement and shortening amount of landmarks with different internal friction angle φ when the rotation angles are 20°. The lateral displacement gets slightly larger as the internal friction angle φ gets larger, except when X = -21.The position where the maximum shortening amount appears does not change apparently, which is still located at the margin of the blocking block (between X = 0 and X = 6 in Fig.S4b). The shortening amount shows no significant difference with various internal friction angle φ.

Table S1. Calcite U-Pb dating results with errors.

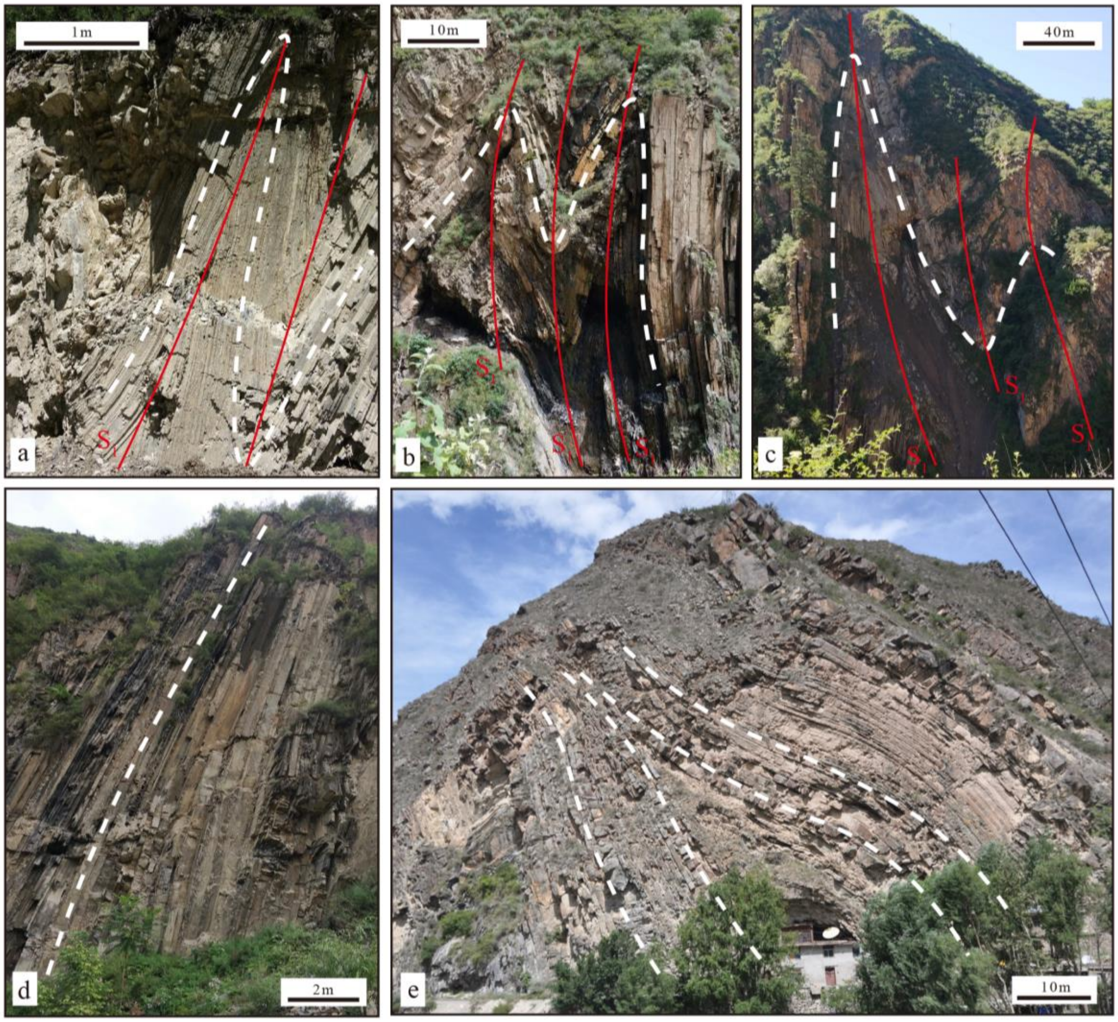

Figure S1. Structures within the Xiaojin Arcuate Zone. (a-c) tight folds with sub-vertical axial planes (S_1); (d) sub-vertical strata; (e) fault-bend folds.

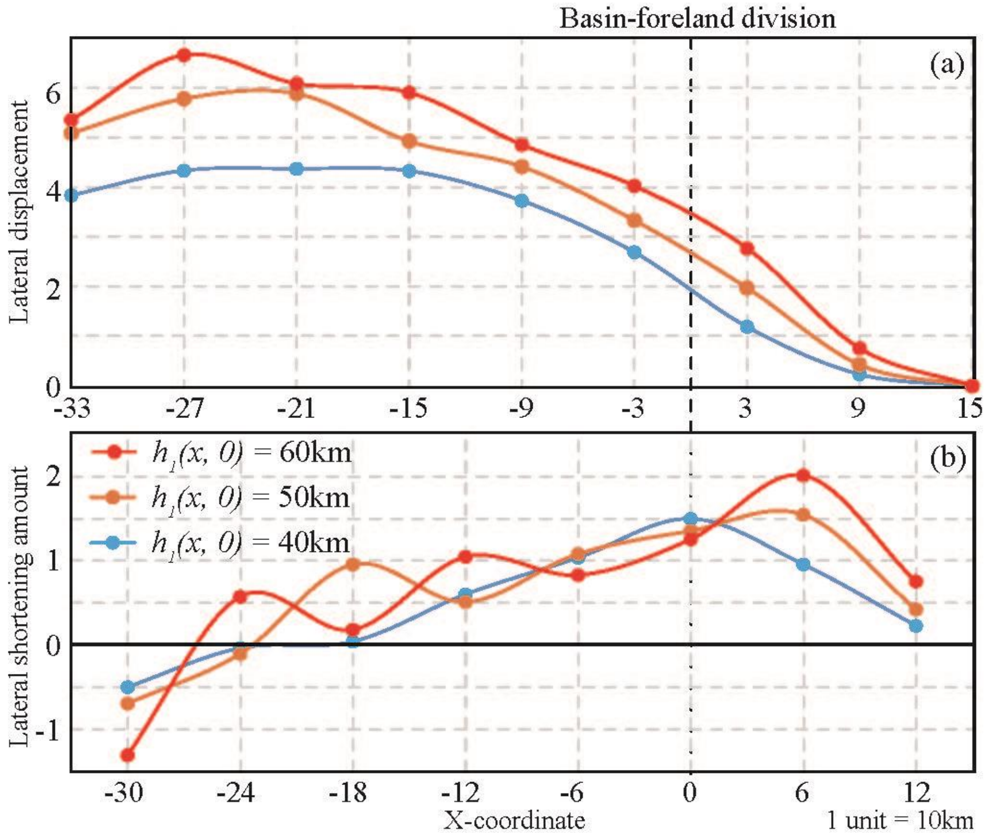

Figure S2. The average lateral displacement and shortening amount in the X direction of landmarks with different X coordinates with different material thickness $h_1(x, 0)$ when the rotation angles are 20°.

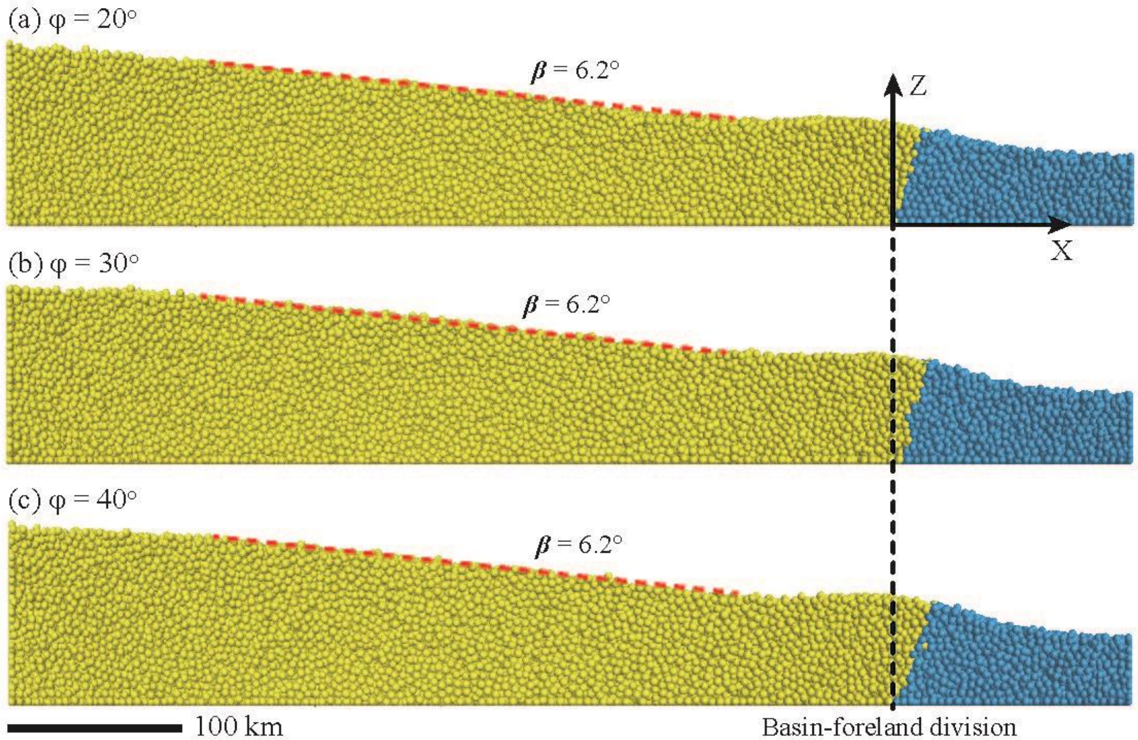

Figure S3. The cross-sectional view (X-Z plane) of the simulation results with different internal friction angle φ when the rotation angles are 20 °.

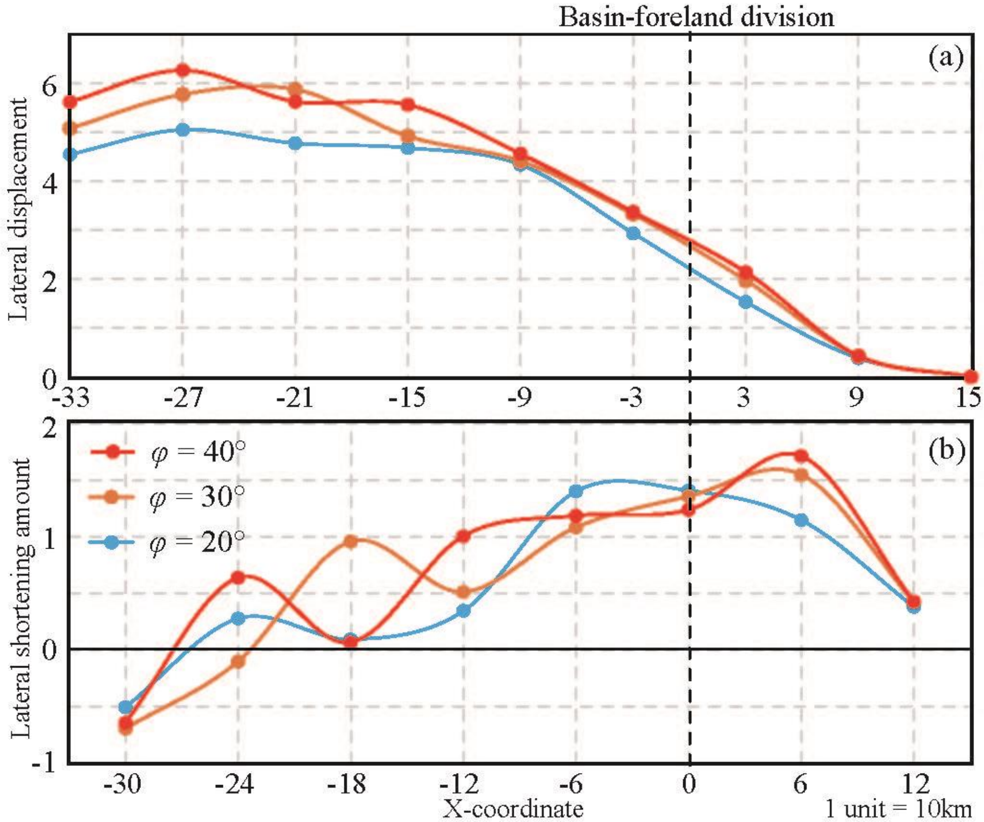

Figure S4. The average lateral displacement and shortening amount in the X direction of landmarks with different X coordinates with different internal friction angle φ when the rotation angles are 20°.

Table S1. Calcite U-Pb dating results with errors.

Spot	Atomic ratios			
	$^{206}Pb^{*}/^{238}U$	±1σ	$^{207}Pb^{*}/^{206}Pb$	±1σ
Sample (CV1)				
CV1_s01	0.30281	0.01229	0.82300	0.01600
CV1_s02	0.45055	0.01632	0.82900	0.01950
CV1_s03	2.79235	0.07942	0.80000	0.02500
~~CV1_s04~~	~~3.95188~~	~~0.18420~~	~~0.89000~~	~~0.05500~~
~~CV1_s05~~	~~4.16359~~	~~0.20446~~	~~0.97000~~	~~0.08000~~
~~CV1_s06~~	~~1.63622~~	~~0.14353~~	~~0.96000~~	~~0.06000~~
~~CV1_s07~~	~~16.68416~~	~~0.85062~~	~~-140.00000~~	~~70.00000~~
CV1_s08	0.84786	0.05010	0.82700	0.03250
CV1_s09	13.19157	0.74634	0.52900	0.04400
~~CV1_s10~~	~~2.58350~~	~~0.08230~~	~~0.90800~~	~~0.02950~~
CV1_s11	0.28092	0.01015	0.85500	0.01300
CV1_s12	0.79713	0.04088	0.82400	0.02200
CV1_s13	0.46867	0.02120	0.85900	0.02000
CV1_s14	1.07448	0.04890	0.86200	0.03050
CV1_s15	9.19768	0.37190	0.75200	0.04400
~~CV1_s16~~	~~7.81764~~	~~0.31454~~	~~1.00000~~	~~0.08000~~
CV1_s17	1.15141	0.07107	0.81600	0.02600
CV1_s18	1.06345	0.04850	0.85800	0.03150
CV1_s19	29.98857	0.81962	0.18600	0.01500
~~CV1_s20~~	~~15.70109~~	~~0.72690~~	~~0.71000~~	~~0.10000~~
CV1_s21	2.51387	0.10503	0.84100	0.03950
CV1_s22	1.21438	0.04427	0.86000	0.03300
CV1_s23	0.81811	0.04665	0.83100	0.02750
CV1_s24	1.04792	0.05887	0.84100	0.02950
CV1_s25	7.58247	0.27433	0.77600	0.03550
Sample (CV2_1)				
CV2_1_s01	33.30873	1.30856	0.22400	0.03050
~~CV2_1_s02~~	~~16.71406~~	~~0.71888~~	~~0.67100~~	~~0.04500~~
CV2_1_s03	10.49093	0.41893	0.77000	0.06000
~~CV2_1_s04~~	~~24.47886~~	~~1.12436~~	~~0.58000~~	~~0.05500~~

~~CV2_1_s05~~	~~8.25349~~	~~0.47476~~	~~-120.00000~~	~~70.00000~~
CV2_1_s06	25.97895	0.79601	0.38000	0.03150
CV2_1_s07	36.14901	1.26101	0.13800	0.01400
CV2_1_s08	23.31611	0.75777	0.37500	0.02150
~~CV2_1_s09~~	~~12.89965~~	~~0.66015~~	~~-200.00000~~	~~85.00000~~
~~CV2_1_s10~~	~~28.52124~~	~~1.22109~~	~~0.44000~~	~~0.09500~~
CV2_1_s11	4.73424	0.25233	0.73400	0.02900
CV2_1_s12	12.45186	0.58186	0.69000	0.07500
CV2_1_s13	0.42587	0.01264	0.83400	0.01150
CV2_1_s14	0.76446	0.02663	0.83800	0.01300
CV2_1_s15	0.43786	0.01233	0.83700	0.01250
CV2_1_s16	29.05435	1.53870	0.37000	0.04750
CV2_1_s17	26.05152	0.98239	0.26300	0.03500
CV2_1_s18	32.72437	1.09081	0.20900	0.02100
CV2_1_s19	3.74556	0.13538	0.77700	0.02550
CV2_1_s20	34.93050	1.37367	0.10800	0.01450
~~CV2_1_s21~~	~~25.55190~~	~~2.41518~~	~~-670.00000~~	~~160.00000~~
CV2_1_s22	3.01827	0.13675	0.84000	0.06000
CV2_1_s23	4.27819	0.24531	0.81000	0.06000
CV2_1_s24	4.12675	0.13695	0.84900	0.03100
~~CV2_1_s25~~	~~3.64314~~	~~0.17789~~	~~0.98000~~	~~0.07500~~